Nonlinear optical phenomena on rough surfaces of metal thin films

Evgeni Y. Poliakov, Vadim A. Markel,* and Vladimir M. Shalaev†
Department of Physics, New Mexico State University, Las Cruces, New Mexico 88003

Robert Botet
Laboratoire de Physique des Solides, Université Paris-Sud, Center d'Orsay, 91405 Orsay Cedex, France
(Received 20 October 1997)

Nonlinear optical phenomena on rough self-affine metal surfaces are theoretically studied. Placing nonlinearly polarizable molecules on such surfaces results in strong enhancement of optical nonlinearities. A quasi-static approximation is used to calculate local-enhancement factors for the second and third harmonic generation, degenerate four-wave mixing, and nonlinear Kerr effect. The calculations show that the average enhancement factors on a self-affine surface can be as large as 10^7 and 10^{15} for optical nonlinearities of the second and third order, respectively, with the maximum average enhancement in the infrared spectral range. Strong spatial inhomogeneity of local-enhancement distribution is demonstrated for the second and third harmonic generation. The local enhancement can exceed the average by several orders of magnitude, reaching extremely high values. Sharp peaks in local-field intensities at fundamental and generated frequencies are localized in spatially separated nanometer-sized areas of the film. [S0163-1829(98)01124-2]

I. INTRODUCTION

Electromagnetic properties of inhomogeneous metal nanocomposites, such as rough thin films and colloidal aggregates, have been intensively studied in the past two decades.[1] As many studies indicate,[1–4] nanocomposites often possess geometrical properties of fractal objects (see, for example, Ref. 2). Physical properties of fractal composites are substantially different from those of conventional ordered and disordered media. Recent studies suggest that in many cases rough metal films (e.g., films obtained by atomic deposition onto a low-temperature substrate) have the properties of self-affine fractal structures.[3,4]

Although self-affine structures differ from self-similar fractal objects (to reveal the scale invariance they require two different scaling factors in the surface plane and in the normal direction), optical properties of self-affine thin films are, in many respects, similar to those of fractal aggregates.[5] For example, both fractal aggregates and self-affine films possess a variety of dipolar eigenmodes distributed over a wide spectral range.[5–7] In contrast, for the case of conventional (nonfractal) random ensembles of monomers, such as a gas of particles or randomly close-packed spheres, the absorption spectra are peaked near a relatively narrow resonance of an individual particle. In fractals, a variety of dipolar eigenmodes can be excited by a homogeneous electric field, whereas only one dipolar eigenmode can be excited in a small dielectric sphere.[8] These striking differences are explained by localization of optical modes in various random, spatially separated, parts of a fractal object.[6,7]

In random but homogeneous media, dipolar modes are, typically, delocalized over large spatial areas. All monomers absorb light energy with approximately equal rate in the regions whose linear dimensions significantly exceed the incident-field wavelength. This is, however, not the case for fractal nanocomposites and self-affine films. Optical excitations in fractal objects tend to be localized.[6,7] Due to this localization, and because of a large number of different resonance frequencies corresponding to various local geometrical structures, the fractal optical modes cover a large spectral interval.

The field distributions are extremely inhomogeneous at the rough surfaces of thin films; there are "cold" regions of small local fields and "hot" areas of high local fields. Strong enhancements of a number of optical phenomena in rough metal films[6,9] are associated with much higher values of local fields in the hot spots, where the optical modes are localized.[6]

The approach employed in this paper is based on the discrete dipole approximation (DDA).[10,11] By using the DDA, linear and nonlinear optical properties of fractal aggregates of particles[5–7] and linear optical properties of self-affine films[5,12,13] have been previously studied.

In the present paper, we investigate nonlinear optical effects in self-affine films. For simplicity, we assume that the "seed" nonlinear susceptibility is due to molecules adsorbed on the film surface rather than due to a nonlinearity of the film itself (most of the obtained results, however, are applicable in the latter case as well). We calculate the average enhancement factors for a number of optical phenomena in self-affine films.

It is important to note that the values of generated local signals in the "hot" spots can be by many orders of magnitude larger than the average (over the whole surface) signal. This opens a fascinating possibility of nonlinear optics and spectroscopy of single molecules located in the hot spots of a rough surface. (A similar pattern for the field distribution occurs in random metal-dielectric films near the percolation.[14]) To demonstrate strongly inhomogeneous character of fields on a rough surface, we calculate the spatial distributions for the local-field intensities at the fundamental frequency and for the generated nonlinear signals. Whereas the average enhancement can be probed by means of conventional far-zone optics, to study the local distribu-

tions of the fields at the fundamental and the generated frequencies one can use the near-field scanning optical microscopy[15] that allows sub-wavelength resolution.

II. GENERAL APPROACH AND REVIEW OF THE DISCRETE DIPOLE APPROXIMATION

The discrete dipole approximation was originally suggested by Purcell and Pennypacker[10] and developed in later papers[11,16–18] to calculate optical responses from an object of an arbitrary shape. It is based on replacing an original dielectric medium by an array of pointlike elementary dipoles. The DDA has been also applied to fractal clusters built from a large number of small interacting monomers.[6,7,19,20] Below we briefly recapitulate the DDA and the related methods based on solving the coupled-dipole equations.[5–7]

Following the main idea of the DDA, we treat a self-affine film as a collection of N identical polarizable particles (monomers) possessing a linear scalar polarizability α. When irradiated by a plane monochromatic incident wave of the form

$$\mathbf{E}_{inc}(\mathbf{r},t) = \mathbf{E}_0 \exp(i\mathbf{k}\cdot\mathbf{r} - i\omega t), \qquad (1)$$

the monomers interact with the incident field and with each other through induced-dipole moments. The local electric field $\mathbf{E}_i$ at the monomer's position $\mathbf{r}_i$ is given by the sum of the incident wave and all the scattered (secondary) waves: $\mathbf{E}_i = \mathbf{E}_{inc}(\mathbf{r}_i,t) + \mathbf{E}_{sc}(\mathbf{r}_i,t)$. The dipole moment $\mathbf{d}_i$ at the ith site is determined as

$$\mathbf{d}_i = \alpha \mathbf{E}_i. \qquad (2)$$

The field $\mathbf{E}_{sc}(\mathbf{r}_i)$, scattered from all other dipoles, generally, contains the near-, intermediate-, and far-zone terms. In this paper, we restrict our consideration to the quasi-static limit, i.e., the characteristic system size L is assumed to be much smaller than the wavelength $\lambda = 2\pi c/\omega$. In this approximation, we leave only the near-field term in the expression for $\mathbf{E}_{sc}(\mathbf{r}_i)$ and the factor $\exp(i\mathbf{k}\cdot\mathbf{r}_i)$ is always close to unity. In addition, the time dependence, $\exp(-i\omega t)$, is the same for all time-varying fields, so that the whole exponential factor can be omitted. After that, the coupled-dipole equations (CDE) for the induced dipoles acquire the following form:[6,7]

$$d_{i,\alpha} = \alpha \left(E_{0,\alpha} + \sum_{j\neq i} W_{ij,\alpha\beta} d_{j,\beta} \right), \qquad (3)$$

$$W_{ij,\alpha\beta} = (3 r_{ij,\alpha} r_{ij,\beta} - \delta_{\alpha\beta} r_{ij}^2)/r_{ij}^5, \qquad (4)$$

where $W_{ij,\alpha\beta}$ is the quasistatic interaction operator between two dipoles, $\mathbf{r}_i$ is the radius vector of the ith monomer, and $\mathbf{r}_{ij} = \mathbf{r}_i - \mathbf{r}_j$. The Greek indices denote Cartesian components of vectors and should not be confused with the polarizability, α. Hereafter, summation over repeated Greek indices is implied, except if stated otherwise.

We model a self-affine film by point dipoles placed according to an algorithm described below in sites of a simple cubic lattice with a period a_0. The occupied sites correspond to the spatial regions filled by the film, while empty sites correspond to the structural voids. The linear polarizability of an elementary dipole (monomer) α is given by the

Lorenz-Lorentz formula having the same form as the polarizability of a dielectric sphere with radius $R_m = (3/4\pi)^{1/3} a_0$ (see, for example, Ref. 21):

$$\alpha = R_m^3 [(\epsilon - 1)/(\epsilon + 2)], \qquad (5)$$

where $\epsilon = \epsilon' + i\epsilon''$ is the bulk dielectric permittivity of the film material. The choice of the sphere radius R_m provides equality of the cubic-lattice elementary-cell volume (a_0^3) and the volume of an imaginary sphere (monomer) that represents a pointlike dipole ($4\pi R_m^3/3$).[10,11,17] Consequently, for large films consisting of many elementary dipoles, the volume of the film is equal to the total volume of the imaginary spheres. Since $a_0 < 2R_m$, the neighboring spheres intersect geometrically. The model of the effective intersecting spheres allows one to take approximately into account the effects of the multipolar interaction within the pure-dipole approximation.[6]

Since $W_{ij,\alpha\beta}$ is independent of the frequency ω in the quasistatic approximation, the spectral dependence of solutions to Eq. (3) is manifested only through $\alpha(\omega)$. For convenience, we introduce the variable $Z(\omega) \equiv 1/\alpha(\omega) = -[X(\omega) + i\delta(\omega)]$. Using Eq. (5), we obtain

$$X \equiv -\mathrm{Re}[\alpha^{-1}] = -R_m^{-3}[1 + 3(\epsilon' - 1)/|\epsilon - 1|^2], \qquad (6)$$

$$\delta \equiv -\mathrm{Im}[\alpha^{-1}] = 3R_m^{-3}\epsilon''/|\epsilon - 1|^2. \qquad (7)$$

The variable X indicates the proximity of ω to an individual particle resonance and plays the role of a frequency parameter; δ characterizes dielectric losses. The resonance quality factor is proportional to δ^{-1}. One can find $X(\lambda)$ and $\delta(\lambda)$ for a specific material using theoretical or experimental data for $\epsilon(\lambda)$ and formulas (6) and (7). In Figs. 1(a) and 1(b), we plot X and δ as functions of the wavelength λ for silver particles[22] ($a_0 = 1$ units are used). As seen, X changes significantly from 400 nm to 800 nm and then, for longer wavelengths, remains almost constant, $X \approx -a_0^3/R_m^3 = -4\pi/3$. The relaxation constant δ is small in the visible spectral range and decreases toward the infrared.

Now we write Eq. (3) in a matrix form. Following Refs. 6 and 7, we introduce a $3N$-dimensional vector space R^{3N} and an orthonormal basis $|i\alpha\rangle$. The $3N$-dimensional vector of dipole moments is denoted by $|d\rangle$, and the incident field is denoted by $|E_{inc}\rangle$. The Cartesian components of three-dimensional vectors $\mathbf{d}_i$ and $\mathbf{E}_{inc}$ are given by $\langle i\alpha|d\rangle = d_{i,\alpha}$ and $\langle i\alpha|E_{inc}\rangle = E_{0,\alpha}$. The last equality follows from the assumption that the incident field is uniform throughout the film. The matrix elements of the interaction operator are defined by $\langle i\alpha|\hat{W}|j\beta\rangle = W_{ij,\alpha\beta}$. Then Eq. (3) can be written as

$$[Z(\omega) - \hat{W}]|d\rangle = |E_{inc}\rangle. \qquad (8)$$

The interaction operator $\hat{W}$ in Eq. (8) is real and symmetrical, as it can be easily seen from the expression (4) for its matrix elements.

By diagonalizing the interaction matrix $\hat{W}$ with $\hat{W}|n\rangle = w_n|n\rangle$ and expanding the $3N$-dimensional dipole vectors in terms of the eigenvectors $|n\rangle$ (as $|d\rangle = \Sigma_n C_n|n\rangle$), we ob-
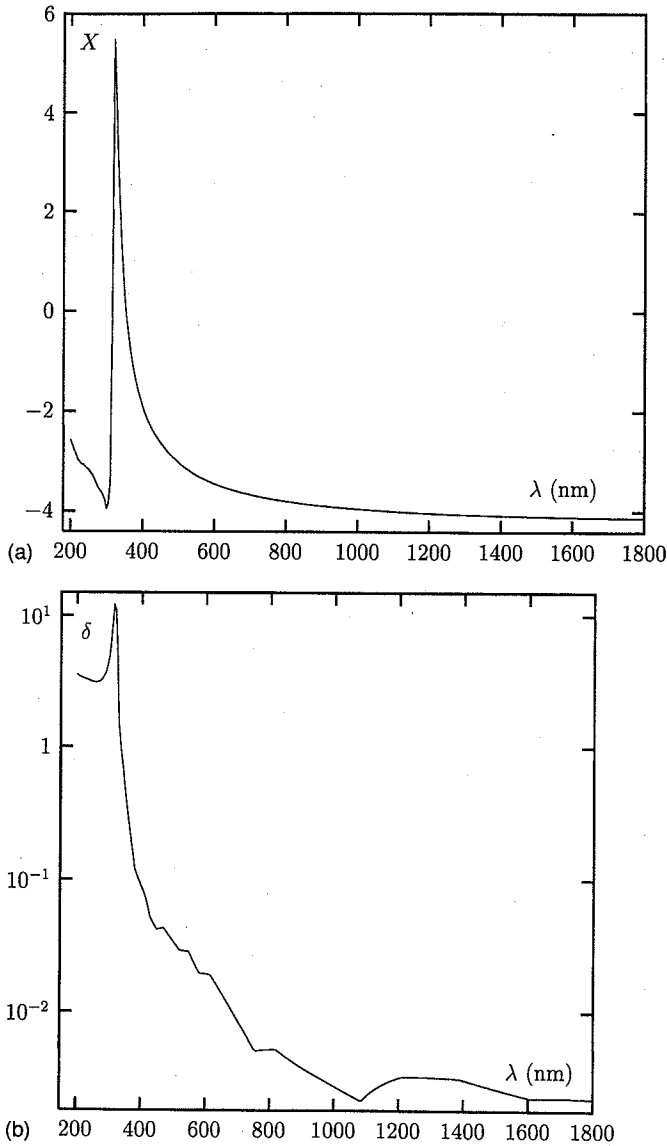
FIG. 1. Spectral dependence of the frequency parameter X and loss parameter δ for silver.

tain a relation between the local fields and the amplitudes of linear dipoles induced by the incident wave (1):[6,7]

$$E_{i,\alpha} = \alpha^{-1} d_{i,\alpha} = Z(\omega)\alpha_{i,\alpha\beta}E_{0,\beta}, \qquad (9)$$

where we introduced the polarizability tensor of the ith dipole, $\hat{\alpha}_i(\omega)$, with its matrix elements $\alpha_{i,\alpha\beta}$ given by

$$\alpha_{i,\alpha\beta} \equiv \alpha_{i,\alpha\beta}(\omega) = \sum_{j,n} \frac{\langle i\alpha|n\rangle\langle n|j\beta\rangle}{Z(\omega)-w_n}. \qquad (10)$$

We note that the only source of dependence on material properties in solution (10) is $Z(\omega) = 1/\alpha(\omega)$; the eigenvectors and eigenvalues of the operator $\hat{W}$ depend only on the film's geometry. For any given dielectric function $\epsilon(\lambda)$, one can calculate the dipole moment components by simple summation according to Eq. (9), provided the eigenvectors and the eigenvalues are known:[6,7]

$$d_{i,\alpha} = \sum_n \frac{\langle i\alpha|n\rangle\langle n|E_{inc}\rangle}{Z(\omega)-w_n} = \sum_{n,j} \frac{\langle i\alpha|n\rangle\langle n|j\beta\rangle}{Z(\omega)-w_n}E_{0,\beta}. \qquad (11)$$

As mentioned in Sec. I, strong spatial fluctuations of the local fields lead to huge enhancements for a number of optical effects in nanocomposites.[5,6,12,13] For optical processes considered below, the enhancement of local fields associated with the dipole-dipole interactions in a film is characterized by the interaction operator $\hat{W}$ in Eq. (4). The induced nonlinear dipoles can have different relative phases. Because we are interested in the average generated nonlinear signal, we sum up the amplitudes of the generated signal over all the points in a film. The average enhancement of the generated signal for coherent nonlinear optical processes can be characterized by the following factor:

$$G = \frac{|\langle \mathbf{D}^{NL}(\omega_g)\rangle|^2}{|\mathbf{D}_0^{NL}(\omega_g)|^2}, \qquad (12)$$

where $\langle \mathbf{D}^{NL}\rangle$ is the average surface-enhanced dipole moment of the nonlinear molecules when they are adsorbed on a film surface, and $\langle \mathbf{D}_0^{NL}\rangle$ is the dipole moment of the same molecules in vacuum.

Note that a definition of the enhancement is arbitrary to some extent. In some cases it is more convenient to define the enhancement in terms of work done by a linearly polarized probe field, $\mathbf{E}_0(\omega_g)$, at the generated frequency ω_g on a self-affine film and in vacuum, $\mathbf{D}^{NL}\cdot\mathbf{E}_0(\omega_g)$ and $\mathbf{D}_0^{NL}\cdot\mathbf{E}_0(\omega_g)$, respectively, i.e., as

$$G = \frac{|\langle \mathbf{D}^{NL}(\omega_g)\cdot\mathbf{E}_0(\omega_g)\rangle|^2}{|\langle \mathbf{D}_0^{NL}(\omega_g)\cdot\mathbf{E}_0(\omega_g)\rangle|^2}. \qquad (13)$$

The probe *linear* field $\mathbf{E}_0(\omega_g)$ should not be confused with the generated field $\mathbf{E}_i(\omega_g)$; the former produces the local field at ω_g through the linear relation (9). Note that the enhancement in Eq. (13) does not depend on the magnitude of the probe field $\mathbf{E}_0(\omega_g)$. Formula (13) is convenient because the enhancement factors can be expressed in terms of the local fields only.

III. PROPERTIES OF SELF-AFFINE STRUCTURES

A. General properties of self-affine films

Surfaces formed by condensing atomic beams onto a low-temperature substrate are characterized by microscopic surface roughness[3] and belong to the Kardar-Parisi-Zhang universality class.[23] Rough-surface profiles exhibit the properties of self-affine fractal structures,[3,4] which reveal their scale-invariance properties when different scaling factors are applied in the plane of the film and in the normal growth direction z. Contrary to the case of "usual" roughness, there is no correlation length for self-affine surfaces, which implies that inhomogeneities of all scales are present (within a certain size interval) according to a power-law distribution. A self-affine surface contains roughness features of very small (asymptotically zero) radii of curvature, i.e., the profile's derivatives can be very large. However, this kind of divergence is only formal, because the scale invariance is
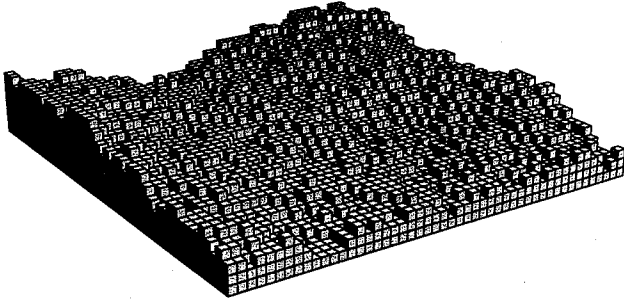
FIG. 2. Self-affine thin film obtained in the RSS model.

valid in the intermediate asymptote region, i.e., on the scales between the size of the smallest roughness features and the size of a sample.

B. Numerical models for rough films

To model a self-affine rough film, we use the restricted solid-on-solid (RSS) model.[24,25] In this model, we add a particle in a growing sample only if the newly created interface does not have steps higher than the lattice period a_0. The surface structure of the generated film does not have overhangs or steps higher than one lattice unit, and a true scaling behavior is clearly pronounced, even for relatively small film sizes. Initially, we generated 12 different random films with a large ($\sim 10^6$) number of sites that allowed us to achieve the scaling condition for the height distribution

$$\langle [h(\mathbf{r}+\mathbf{R})-h(\mathbf{r})]^2 \rangle \approx R^{2D_H}, \qquad (14)$$

where $\mathbf{R}$ is the vector in the plane of growth, x-y plane, and the scaling exponent D_H is related to the fractal dimension, $D=2.6$, by $D_H=3-D$. The expression in the left-hand side of formula (14) is known as the height-height correlation function. In Fig. 2, we show a typical self-affine film generated in the RSS model, after removing the regular part at the bottom (see below).

The analysis demonstrated in Sec. II requires the knowledge of all the eigenstates and eigenvalues of the matrix $W_{ij,\alpha\beta}$. We stored all the eigenvalues and eigenfunctions in order not to repeat time-consuming calculations of the local polarizabilities in Eq. (10) for each wavelength. To diagonalize $W_{ij,\alpha\beta}$, we used the Householder algorithm.

For calculating nonlinear optical responses, we restricted our model to an average number of $N \sim 10^3$ monomers per film sample (cluster). To make the reduction of the number of particles, we cut a "parent" cluster. The "excess" monomers that represent a regular part at the bottom of the film were removed, so that the resultant sample had at least one hole. Note that such a procedure does not change the scaling properties (14) of the surface. As a result, the total number of monomers left was in the interval $(\langle N \rangle - \sigma_N, \langle N \rangle + \sigma_N)$, where σ_N is a constant.

Twelve nearly monodisperse samples with monomers distributed on a 14×14 surface lattice were used for most of our numerical calculations. The lattice unit was chosen to be $a_0 \sim 5$ nm and the inequality $L < \lambda$ was fulfilled, i.e., the quasistatic approximation was valid.

The actual characteristics of the "14×14" ensemble of 12 films were as follows: total number of monomers, N

$=8271$, providing $\langle N \rangle = N/12 \approx 690$ and $\sigma_N = 110$, the average number of monomers occupying the surface, $\langle N_S \rangle = 218$ so that $\langle N_S \rangle / \langle N \rangle \approx 1:3$: None of the clusters was composed of more than five adjacent monomer layers.

IV. SECOND-ORDER NONLINEAR EFFECTS

In this section, we consider the second harmonic generation[26,27] (SHG) as a typical example of nonlinear optical phenomena of the second order. Because SHG is extremely sensitive to the surface roughness conditions (which made it a widely used technique for studying structural and electronic properties of surfaces and interfaces[27-29]), this process is of fundamental importance for understanding the nonlinear interaction of light with self-affine films.

A. SHG from noncentrosymmetric molecules on a self-affine surface

For SHG, the nonlinear polarization $\mathbf{P}^{(2)}(2\omega)$ is commonly introduced through the definition of the nonlinear susceptibility surface tensor of a third rank $\hat{\chi}^{(2)}(2\omega;\omega,\omega)$ as

$$\mathbf{P}^{(2)}(2\omega) = \hat{\chi}^{(2)}(2\omega;\omega,\omega):\mathbf{E}(\omega):\mathbf{E}(\omega). \qquad (15)$$

Extensive studies of different mechanisms of SHG on surfaces[30,31] and in bulk[32,33] have been carried out for jellium and other models since they were first proposed by Rudnick and Stern.[34] In this paper, we assume that contributions to $\hat{\chi}^{(2)}$ are associated with adsorbed molecules placed on the film's surface. The nonlocal effects (related to the spatial dispersion) and the effects of finite depth field penetration are left out of the analysis.

We adopt the following asymmetrical structure for the nonlinear absorbed molecules. They are assumed to have a "preferred" direction $\mathbf{n}$ that coincides with the normal vector to the (x,y) plane of the film, so that the film anisotropy is reproduced by the adsorbed molecules.[35]

We construct the vector $\mathbf{P}^{(2)}(2\omega)$ from the obvious independent combinations of the triplet $(\mathbf{n},\mathbf{E},\mathbf{E})$ in Eq. (15):

$$\mathbf{P}^{(2)}(2\omega) = A(\mathbf{E} \cdot \mathbf{E})\mathbf{n} + B(\mathbf{n} \cdot \mathbf{E})\mathbf{E}, \qquad (16)$$

where A and B are two independent complex constants determined only by the internal structure of the molecules absorbed on the surface (they are not related to the parameters a and b originally introduced by Rudnick and Stern in Ref. 34 and frequently used in the literature on the SHG).

Comparing the components of the polarization vector given in Eq. (15) with the ones introduced in Eq. (16), we obtain the following relations for the nonzero components of $\hat{\chi}^{(2)}$:

$$\chi^{(2)}_{xxz} = \chi^{(2)}_{xzx} = \chi^{(2)}_{yzy} = \chi^{(2)}_{yyz} = B,$$

$$\chi^{(2)}_{zxx} = \chi^{(2)}_{zyy} = A, \qquad \chi^{(2)}_{zzz} = A+B. \qquad (17)$$

The amplitude of a nonlinear dipole located at ith site can be written in a form similar to Eq. (16) as

$$\mathbf{d}^{NL}_i = a(\mathbf{E}_i \cdot \mathbf{E}_i)\mathbf{n} + b(\mathbf{n} \cdot \mathbf{E}_i)\mathbf{E}_i, \qquad (18)$$

where $a = Av, b = Bv, v = 4\pi R_m^3/3$, and $\mathbf{E}_i$ is the local field.

First, we find the average nonlinear dipole moment for the nonlinear molecules on the plane with $\epsilon \approx 1$ (in vacuum), $\langle \mathbf{D}_0^{NL} \rangle$. In this case, the induced dipoles are excited only by the uniform incident field $\mathbf{E}_0$ so that $\mathbf{E}_i = \mathbf{E}_0$. It follows from Eq. (18) that

$$\langle \mathbf{D}_0^{NL} \rangle = a(\mathbf{E}_0 \cdot \mathbf{E}_0)\mathbf{n} + b(\mathbf{n} \cdot \mathbf{E}_0)\mathbf{E}_0. \qquad (19)$$

Vector $\mathbf{P}^{(2)}(2\omega)$ strongly depends on the incident polarization (see, for example, Refs. 5 and 12). In this paper, we assume that an incident wave (1) is linearly polarized, unless noted otherwise. Then

$$|\langle \mathbf{D}_0^{NL} \rangle|^2 = \{|a|^2 + [|b|^2 + 2\,\mathrm{Re}(ab^*)]\cos^2(\theta)\}|\mathbf{E}_0|^4, \qquad (20)$$

where the asterisk denotes complex conjugation, and θ is the angle between the z axis and the direction of $\mathbf{E}_0$.

When the incident wave is polarized along the z axis (that hereafter we refer to as p polarization) or in the (x,y) plane (s polarization), expression (20) simplifies to

$$|\langle \mathbf{D}_0^{NL} \rangle|^2 = |\mathbf{E}_0|^4 |a + b|^2, \quad p \text{ polarization}, \qquad (21)$$

$$|\langle \mathbf{D}_0^{NL} \rangle|^2 = |\mathbf{E}_0|^4 |a|^2, \quad s \text{ polarization}. \qquad (22)$$

Because the induced nonlinear dipoles on surface can interact with each other via the *linear* polarizabilities $\alpha(2\omega)$, we can write an analog of the CDE in Eq. (3) for the nonlinear dipole amplitudes as

$$\mathbf{d}_i^{NL} = v\hat{\chi}^{(2)}(2\omega;\omega,\omega){:}\mathbf{E}_i^2(\omega) + \alpha(2\omega)\sum_{j \neq i} \hat{W}_{ij}\mathbf{d}_j^{NL}(2\omega) \qquad (23)$$

and its matrix counterpart

$$|d^{NL}\rangle = v|\hat{\chi}^{(2)}{:}E^2\rangle + \alpha(2\omega)\hat{W}|d^{NL}\rangle, \qquad (24)$$

where

$$v\langle i\alpha|\hat{\chi}^{(2)}{:}E^2\rangle = an_\alpha E_{i\beta}E_{i\beta} + bn_\beta E_{i\alpha}E_{i\beta}. \qquad (25)$$

In Eqs. (23) and (24), we included the linear interaction of the local nonlinear dipoles at the double frequency 2ω; this provides an additional contribution to the nonlinear SHG signal (cf. Eq. 18).

B. Interaction of linear dipoles in a cluster

First, we take into account only interactions of linear dipoles at the fundamental frequency ω and ignore the dipole interactions at the generated frequency 2ω. This is justified when the frequency 2ω is out of resonance with any of the surface eigenmodes (at the same time, the fundamental frequency ω can be within the resonance band). Then Eq. (23) reduces to Eq. (18). Using Eqs. (18) and (2), we obtain

$$|\langle \mathbf{D}^{NL} \rangle|^2 = |Z(\omega)|^4 \{|a\langle d^2 \rangle|^2 + 2\,\mathrm{Re}[ab^*\langle d^2 \rangle \langle d_z^2 \rangle^*]$$
$$+ |b\langle d_z \mathbf{d} \rangle|^2\}, \qquad (26)$$

$$\langle d^2 \rangle = (1/N_S)\sum_{i \in S} (\mathbf{d}_i \cdot \mathbf{d}_i), \qquad (27)$$

$$\langle d_z^2 \rangle = (1/N_S)\sum_{i \in S} (\mathbf{d}_i \cdot \mathbf{n})^2, \qquad (28)$$

$$\langle \mathbf{d}d_z \rangle = (1/N_S)\sum_{i \in S} \mathbf{d}_i(\mathbf{d}_i \cdot \mathbf{n}), \qquad (29)$$

where $\mathbf{d}$ (and related quantities) in Eqs. (26)–(29) refer to linear dipoles, and N_S is the total number of surface monomers.

Since a self-affine film is, on average, isotropic in the x-y plane, we adopt the following approximation (verified also by our numerical simulations): $|\langle \mathbf{d}d_z \rangle| \approx |\langle d_z^2 \rangle|$ for the s and p polarizations of the incident wave. Note that the same approximation was used in Ref. 36. Then Eq. (26) takes the form

$$|\langle \mathbf{D}^{NL} \rangle|^2 = |Z(\omega)|^4 |(a + b)\langle d_z^2 \rangle + a\langle d_x^2 + d_y^2 \rangle|^2. \qquad (30)$$

Using Eq. (2) and $Z = 1/\alpha$, we rewrite Eq. (30) in terms of the local fields $\mathbf{E}_i$:

$$|\langle \mathbf{D}^{NL} \rangle|^2 = |(a + b)\langle E_z^2 \rangle + a\langle E_x^2 + E_y^2 \rangle|^2. \qquad (31)$$

Now we substitute Eqs. (21), (22), and (31) into Eq. (12) to obtain the enhancement factors for the p and s polarizations:

$$G_{SHG} = |\langle E_z^2 \rangle + \Gamma^{-1}\langle E_x^2 + E_y^2 \rangle|^2/|\mathbf{E}_0|^4, \quad p \text{ polarization}, \qquad (32)$$

$$G_{SHG} = |\Gamma\langle E_z^2 \rangle + \langle E_x^2 + E_y^2 \rangle|^2/|\mathbf{E}_0|^4, \quad s \text{ polarization}, \qquad (33)$$

where the oblique coefficient Γ is defined with the use of Eq. (17) as

$$\Gamma \equiv \frac{\chi_{zzz}^{(2)}}{\chi_{zxx}^{(2)}} = \frac{\chi_{zzz}^{(2)}}{\chi_{zyy}^{(2)}} = 1 + b/a. \qquad (34)$$

C. Interaction of nonlinear dipoles at double frequency

The interactions of nonlinear dipoles at the generated frequency 2ω become important, if this frequency is within the surface mode band. In this case the local fields at both the fundamental and generated frequencies can excite the resonant surface modes and thus get strongly enhanced. Accordingly, the resultant enhancement can become much larger than for the case without interaction of nonlinear dipoles. In order to take into account the coupling of nonlinear dipoles, we must use Eq. (23). A formal solution to a similar equation for linear dipole moments (8) was given in Sec. II [see Eq. (11)]. It can be easily generalized for the case of the coupled nonlinear dipoles (24):

$$|d^{NL}\rangle = vZ(2\omega)\sum_n \frac{|n\rangle\langle n|\hat{\chi}^{(2)}{:}E^2\rangle}{Z(2\omega) - w_n}, \qquad (35)$$

where $Z(2\omega) \equiv \alpha^{-1}(2\omega)$ and $\alpha(2\omega)$ is the scalar polarizability of a monomer at the double frequency.

Using definition (25) of $|\hat{\chi}^{(2)}{:}E^2\rangle$ together with Eqs. (35) and (9), we express the Cartesian components of the average nonlinear dipole moment $\langle \mathbf{D}^{NL}(2\omega) \rangle$ as

$$\langle D_\alpha^{NL} \rangle = Z(2\omega)Z^2(\omega)[(a+b)\langle \alpha_{z\alpha}d_z^2 \rangle + a\langle \alpha_{z\alpha}(d_x^2+d_y^2)\rangle$$
$$+ b\langle \alpha_{x\alpha}d_x d_z + \alpha_{y\alpha}d_y d_z \rangle], \tag{36}$$

where $\alpha_{\alpha\beta} \equiv \alpha_{\alpha\beta}(\omega_g)$ is the local linear polarizability at the generated frequency ω_g. [For simplicity, we omit the argument 2ω for $\alpha_{\alpha\beta}(\omega_g)$ in Eq. (36).] The linear polarizability at the generated frequency is defined similarly to Eq. (10) as

$$\alpha_{i,\alpha\beta}(\omega_g) = \sum_{j,n} \frac{\langle i\alpha|n\rangle\langle n|j\beta\rangle}{Z(\omega_g)-w_n}, \quad i \in S. \tag{37}$$

Here ω_g is the generated signal frequency for the nonlinear process under consideration. The summation over j, i.e., over all the monomers in Eq. (37), is the consequence of the coupling of nonlinear dipoles given by the second term in Eq. (23).

The average (over a film surface) SHG enhancement factor can be obtained by substituting Eqs. (21), (22), and (36) into Eq. (12); with the use of Eq. (2) this gives

$$G_{SHG} = \frac{|Z(2\omega)|^2}{|E_0|^4} \sum_\beta |\langle \alpha_{z\beta}E_z^2 \rangle + \frac{1}{\Gamma}\langle \alpha_{z\beta}(E_x^2+E_y^2)\rangle$$
$$+ \left(1-\frac{1}{\Gamma}\right)\langle \alpha_{x\beta}E_xE_z + \alpha_{y\beta}E_yE_z \rangle|^2,$$

$$p \text{ polarization,} \tag{38}$$

$$G_{SHG} = \frac{|Z(2\omega)|^2}{|E_0|^4} \sum_\beta |\Gamma\langle \alpha_{z\beta}E_z^2 \rangle + \langle \alpha_{z\beta}(E_x^2+E_y^2)\rangle$$
$$+ (\Gamma-1)\langle \alpha_{x\beta}E_xE_z + \alpha_{y\beta}E_yE_z \rangle|^2,$$

$$s \text{ polarization,} \tag{39}$$

where $\alpha_{\alpha\beta} = \alpha_{\alpha\beta}(2\omega)$ is given by Eq. (37) and E_α represents the local-field components.

Note that the above expressions contain the nonlinear polarizability tensor $\hat{\alpha}_i(2\omega)$ and cannot be written only in terms of the local fields E_i. Therefore, if interactions of the generated nonlinear dipoles at frequency ω_g are important, it is impossible to express the enhancement factor in terms of the local and incident fields only. [Compare with Eqs. (32) and (33).]

If we use definition (13) to express the enhancement in terms of work done by a probe field at the generated frequency, then for the case of p polarization, for example, we obtain the following expression

$$G_{SHG} = \frac{1}{|E_0^2 E_0(2\omega)|^2} |\langle E_z(2\omega)E_z^2 \rangle + \frac{1}{\Gamma}\langle E_z(2\omega)(E_x^2+E_y^2)\rangle$$
$$+ \left(1-\frac{1}{\Gamma}\right)\langle E_x(2\omega)E_xE_z + E_y(2\omega)E_yE_z \rangle|^2,$$

$$p \text{ polarization,} \tag{40}$$

where E is the local field at frequency ω, and $E(2\omega)$ is the local *linear* field at 2ω, which is related to the probe field $E_0(2\omega)$ as $E_{i,\alpha}(2\omega) = Z(2\omega)\alpha_{i,\alpha\beta}(2\omega)E_{0,\beta}(2\omega)$ with $\alpha_{i,\alpha\beta}(2\omega)$ defined in Eq. (37). Although the enhancement does not depend on the magnitude of $E_0(2\omega)$; it depends, in

general, on the chosen polarization for $E_0(2\omega)$. Therefore, the above formula can be used only as an approximation to characterize enhancement in terms of the local fields.

Equations (38)–(40) can be simplified to Eq. (32) and (33) when the coupling of nonlinear dipoles is not effective on a surface. As mentioned, it occurs when the generated frequency $\omega_g = 2\omega$ is far from any of the surface eigenmodes, so that $|Z(\omega_g)| \gg w_n, \forall n$. Then the polarizability matrix (37) becomes diagonal: $\alpha_{i,\alpha\beta}(\omega_g) \approx \delta_{\alpha\beta}/Z(\omega_g)$. By applying this to Eqs. (38) and (39) [or, equivalently, setting $E(2\omega) = E_0(2\omega)$ in Eq. (40)], and using the previously adopted approximation $|\langle d_z d_\alpha \rangle| \sim 0, \alpha = x,y$, we obtain Eqs. (32) and (33).

In addition to the average enhancement factors, we calculate spatial distributions of local enhancements on a film surface, $g_{SHG}(\mathbf{r}_i) = |\mathbf{d}_i^{NL}|^2/|\mathbf{d}_0^{NL}|^2$, $i \in S$ in Sec. VI B. The nonlinear local dipoles on a metal self-affine surface, $\mathbf{d}_i^{NL} \equiv \mathbf{d}_i^{NL}(2\omega)$, and in vacuum, $\mathbf{d}_0^{NL} \equiv \mathbf{d}_0^{NL}(2\omega)$, are given by Eq. (35) and Eqs. (25) and (19), respectively.

V. THIRD-ORDER NONLINEAR EFFECTS

In this section, we assume that nonlinear optical susceptibilities are associated with spherically symmetrical molecules adsorbed on a self-affine surface. This means that there is only one independent component for the fourth-rank susceptibility tensor $\chi_{\alpha\beta\gamma\delta}^{(3)}$ that is responsible for the third-order nonlinear optical processes.

A. Third harmonic generation

The spherical symmetry of the adsorbed molecules implies that the amplitudes of the nonlinear dipole moments can be expressed as

$$\mathbf{d}_i^{NL}(3\omega) = c\mathbf{E}_i(\mathbf{E}_i \cdot \mathbf{E}_i), \tag{41}$$

where c is the only independent element of the third-order susceptibility tensor. In Eq. (41), we neglected interactions of the nonlinear dipoles at the frequency 3ω. Using Eq. (41) and replacing $\mathbf{E}_i$ by $\mathbf{E}_0$, we find the denominator in Eq. (12):

$$|\langle \mathbf{D}_0^{NL} \rangle|^2 = |c|^2|\mathbf{E}_0|^6. \tag{42}$$

Interaction of nonlinear dipoles at the frequency $\omega_g = 3\omega$ occurs due to nonzero linear polarizability $\alpha(3\omega)$. This interaction further amplifies amplitudes of the nonlinear dipoles, whose values are given by Eqs. (24) and (25) with $|\hat{\chi}^{(2)}:E^2\rangle$ replaced by $|\hat{\chi}^{(3)}:E^3\rangle$ and 2ω by 3ω, so that we have

$$|d^{NL}\rangle = v|\hat{\chi}^{(3)}:E^3\rangle + \alpha(3\omega)\hat{W}|d^{NL}\rangle, \tag{43}$$

where

$$v\langle i\alpha|\hat{\chi}^{(3)}:E^3\rangle = cE_{i\alpha}E_{i\beta}E_{i\beta}. \tag{44}$$

To solve Eqs. (43) and (44), we can use the formalism of the previous section. The α component of the nonlinear dipole moment, averaged over the surface, is given by

$$\langle D_\alpha^{NL}\rangle = \frac{cZ(3\omega)}{N_S}\sum_{j\in S}\alpha_{j,\beta\alpha}(3\omega)E_{j\beta}E_{j\gamma}E_{j\gamma}, \quad (45)$$

where $Z(3\omega) = \alpha^{-1}(3\omega)$. The nonlinear polarizability matrix for the ith monomer is defined by Eq. (37). It is interesting to note that $\langle D_\alpha^{NL}\rangle$ is, in general, complex, even if c is real, i.e., there is no nonlinear absorption in the system. This property reflects the fact that the average nonlinear dipole moment $\langle \mathbf{D}^{NL}\rangle$ is affected by the surface eigenmodes having finite losses. Also, $\langle \mathbf{D}^{NL}\rangle$ is elliptically polarized because the complex matrix (10) transforms the linear polarization of the incident field into an elliptical polarization of dipole moments [see formula (9)].

Substitution of Eqs. (42) and (45) into Eq. (12) gives the following expression for the surface-enhanced THG in the case of linear polarization of the incident wave:

$$G_{THG} = \frac{|Z(3\omega)|^2}{|E_0|^6}\sum_\gamma |\langle\alpha_{\beta\gamma}(3\omega)E_\beta(\mathbf{E}\cdot\mathbf{E})\rangle|^2. \quad (46)$$

If we use formula (13) for the enhancement factor, it can be expressed in terms of the local fields as

$$G_{THG} = \frac{|\langle[\mathbf{E}(3\omega)\cdot\mathbf{E}](\mathbf{E}\cdot\mathbf{E})\rangle|^2}{|E_0^3 E_0(3\omega)|^2}, \quad (47)$$

where E and $E(3\omega)$ are the local linear fields at frequencies ω and 3ω, induced by the applied field E_0 and the probe field $E_0(3\omega)$, respectively.

If the generated 3ω signal does not excite the surface eigenmodes, so that $\alpha_{\alpha\beta}(3\omega)\approx\delta_{\alpha\beta}/Z(3\omega)$, expression (46) simplifies to

$$G_{THG} = \frac{|\langle\mathbf{E}(\mathbf{E}\cdot\mathbf{E})\rangle|^2}{|E_0|^6}. \quad (48)$$

Analogously to SHG, we also calculate the spatial distributions for local enhancements for THG on a film surface, $g_{THG}(\mathbf{r}_i) = |\mathbf{d}_i^{NL}|^2/|\mathbf{d}_0^{NL}|^2, i\in S$, where $\mathbf{d}_i^{NL}$ and $\mathbf{d}_0^{NL}$ are the local nonlinear dipoles at 3ω on a metal self-affine surface and in a vacuum, respectively.

B. Degenerate four-wave mixing in self-affine films

A typical degenerate four-wave mixing (DFWM) experiment involves two oppositely directed pump beams, $\mathbf{E}_f$ and $\mathbf{E}_b$, and a signal $\mathbf{E}_s$, usually directed at some small angle with respect to the pump beams. All the waves have the same (or close) frequency and differ either in their propagation direction or in polarization (or both).

In the process resulting in the optical phase conjugation, the generated wave $\mathbf{E}_g$ has the same frequency as the pump waves. This feature makes DFWM different from the second and third harmonic generation. In a standard DFWM process, the generated wave propagates against the signal beam, so that the phase matching condition, $\mathbf{k}_f+\mathbf{k}_b+\mathbf{k}_s+\mathbf{k}_g = 0$, is fulfilled.

We consider the total applied field as a superposition of the pump and signal fields:

$$\mathbf{E}_0 = \mathbf{E}_f + \mathbf{E}_b + \mathbf{E}_s. \quad (49)$$

Since the optical nonlinearities are caused by spherically isotropic molecules, the nonlinear polarization can be written as[37]

$$\mathbf{P}^{(3)}(\omega) = A(\mathbf{E}\cdot\mathbf{E}^*)\mathbf{E} + B(\mathbf{E}\cdot\mathbf{E})\mathbf{E}^*/2, \quad (50)$$

where the coefficients A and B are different from those in Sec. IV. When the nonlinear response of the adsorbed molecules is due to nonresonant electronic response (the surface modes, however, can be in resonance with the applied field), A is equal to B.[37] By adopting the condition $A=B$, we write the amplitude of an average nonlinear dipole, induced only by the applied field, as

$$|\langle\mathbf{D}_0^{NL}\rangle| = \tfrac{9}{4}|a|^2|\mathbf{E}_0|^6, \quad (51)$$

where, as above, $a=Av$, and $v=4\pi R_m^3/3$. In Eq. (51), we assumed that E_0 is linearly polarized. For the case of circular polarization, the coefficient in front of $|a|^2$ becomes unity in formula (51). For DFWM, the CDE have the form

$$|d^{NL}\rangle = v|\hat{\chi}^{(3)}:E^3\rangle + \alpha(\omega)\hat{W}|d^{NL}\rangle, \quad (52)$$

$$v\langle i\alpha|\hat{\chi}^{(3)}:E^3\rangle = a(E_{i\alpha}E_{i\beta}E_{i\beta}^* + \tfrac{1}{2}E_{i\alpha}^*E_{i\beta}E_{i\beta}). \quad (53)$$

The exact solution to Eq. (52) is determined by the following formula, valid for any polarization,

$$|\langle\mathbf{D}^{NL}\rangle|^2 = |a|^2|Z(\omega)|^2$$
$$\times\sum_\gamma |\langle\alpha_{\beta\gamma}(\omega)[E_\beta|\mathbf{E}|^2 + \tfrac{1}{2}E_\beta^*(\mathbf{E}\cdot\mathbf{E})]\rangle|^2.$$
$$(54)$$

The final expression for the enhancement factor is formally the same as in Eq. (12) with $|\langle\mathbf{D}_0^{NL}\rangle|^2$ given by Eq. (51) and $|\langle\mathbf{D}^{NL}\rangle|^2$ given by Eq. (54).

Using formula (13), we obtain the following formula for the enhancement

$$G_{DFWM} = \frac{|\langle|\mathbf{E}|^2(\mathbf{E}\cdot\mathbf{E})\rangle|^2}{|E_0|^8}. \quad (55)$$

C. Kerr nonlinearity

In the optical Kerr effect, the nonlinear correction to the refractive index is proportional to the intensity of local electromagnetic field in a medium. For the complex refractive index, $n=n'+in''$, we write

$$n' = n_0' + n_2'I = n_0' + \frac{n_0'c}{2\pi}n_2'|\mathbf{E}|^2, \quad (56)$$

$$\alpha_{abs} = n''\frac{2\omega}{c} = (n_0''+n_2''I)\frac{2\omega}{c}. \quad (57)$$

Here n_0' and $n_0''(2\omega/c)$ are the linear refraction and absorption coefficients, whereas $n_2'I$ and $n_2''I(2\omega/c)$ are the nonlinear corrections to the refraction n' and absorption α_{abs}.

The Kerr-type nonlinear polarization is given by the formula

$$P_\alpha^{(3)}(\omega)=3\chi_{\alpha\beta\gamma\delta}^{(3)}E_\beta E_\gamma^* E_\delta. \qquad (58)$$

The prefactor 3 represents the number of distinct permutations of the frequencies ω, ω, and $-\omega$ of the fields in Eq. (58) (see, for example, Ref. 37). For an isotropic particle, there is only one independent component of $\chi_{\alpha\beta\gamma\delta}^{(3)}$ that we denote simply as $\chi^{(3)}$. Then Eq. (58) simplifies to

$$\mathbf{P}^{(3)}(\omega)=3\chi^{(3)}|E|^2\mathbf{E}. \qquad (59)$$

Note that this expression is similar to the first term in the right-hand side of Eq. (50) for the DFWM process.

The complex refractive index n is related to the susceptibility of the medium χ by $n^2=1+4\pi\chi$, where χ contains, in general, linear and nonlinear terms. For the third-order nonlinearities of the Kerr type, this formula takes the form $n^2=1+4\pi(\chi^{(1)}+3\chi^{(3)}|\mathbf{E}|^2)$.

By considering real and imaginary parts corresponding to the different powers of the electric field in the equality

$$n^2=(n'+in'')^2=1+4\pi(\chi^{(1)}+3\chi^{(3)}|\mathbf{E}|^2), \qquad (60)$$

we obtain the following expressions for the nonlinear corrections to the refractive and absorption:

$$n_2'=\frac{12\pi^2}{n_0'c}\left[\frac{n_0'\text{Re}(\chi^{(3)})+n_0''\text{Im}(\chi^{(3)})}{(n_0')^2+(n_0'')^2}\right] \qquad (61)$$

and

$$n_2''=\frac{12\pi^2}{n_0'c}\left[\frac{n_0'\text{Im}(\chi^{(3)})+n_0''\text{Re}(\chi^{(3)})}{(n_0')^2+(n_0'')^2}\right]. \qquad (62)$$

If the linear absorption is weak ($n_0'\gg n_0''$) but the nonlinear absorption is significant [$|\text{Re}(\chi^{(3)})|\sim|\text{Im}(\chi^{(3)})|$], formulas (61) and (62) can be simplified to the following well-known expressions:

$$n_2'\approx\frac{12\pi^2}{(n_0')^2c}\text{Re}(\chi^{(3)}), \qquad (63)$$

$$n_2''\approx\frac{12\pi^2}{(n_0')^2c}\text{Im}(\chi^{(3)}). \qquad (64)$$

Experimentally, the refractive index change is determined for a sample with characteristic geometrical size much larger than the wavelength. But the quasistatic approximation treats the objects with dimension less than λ. However, we can consider a medium built of many films with linear sizes less than λ (for example, a layered material). Then the resultant size of the medium can be larger than the wavelength so that the refractive index can be introduced in the usual way. The "seed" Kerr susceptibility $\chi^{(3)}$ in such composite material can be strongly enhanced so that the effective nonlinear susceptibility $\chi_{eff}^{(3)}$ of the composite is

$$\chi_{eff}^{(3)}=p\chi^{(3)}G_K, \qquad (65)$$

where p is the volume fraction filled by the films providing the enhancement and G_K is the enhancement factor of the Kerr nonlinearity for an individual film.

Formulas (61)–(64) describe the nonlinear changes in the complex refractive index with account of Eq. (65). The spectra for n_2' and n_2'' can be obtained from λ dependences of G_K (studied below) and $\chi^{(3)}$.

Note that the enhancement factor G_K in Eq. (65) is, in general, complex because of the resonant excitation of the surface eigenmodes having finite losses. If the seed $\chi^{(3)}$ is complex as well, both the real and imaginary parts of G_K contribute to the nonlinear refraction and absorption: $n'=\text{Re}(\chi^{(3)})\text{Re}(G_K)-\text{Im}(\chi^{(3)})\text{Im}(G_K)$ and $n''=\text{Re}(\chi^{(3)})\text{Im}(G_K)+\text{Im}(\chi^{(3)})\text{Re}(G_K)$. If, however, $\chi^{(3)}$ is real, then $n'=\chi^{(3)}\text{Re}(G_K)$ and $n''=\chi^{(3)}\text{Im}(G_K)$.

First, we consider a single arbitrarily oriented film excited by a polarized incident wave. When the scattered fields at the generated frequency are included, a nonlinear dipole moment at the ith site is described by the equation

$$\mathbf{d}_i^{\text{NL}}=c|\mathbf{E}_i|^2\mathbf{E}_i+\alpha(\omega)\sum_{j\neq i}\hat{W}_{ij}\mathbf{d}_j^{\text{NL}}, \qquad (66)$$

where the constant c is related to $\chi^{(3)}$ by $c=v\chi^{(3)}$.

Solving the CDE in Eq. (66) by the method used in Secs. IV and V A, we find the average nonlinear dipole moment $\langle\mathbf{D}^{\text{NL}}\rangle$ with its components $\langle D_\alpha^{\text{NL}}\rangle$ given by

$$\langle D_\alpha^{\text{NL}}\rangle=c|Z(\omega)|^2Z^2(\omega)\langle|d|^2d_\beta\alpha_{\beta\alpha}(\omega)\rangle, \qquad (67)$$

where $\alpha_{i,\alpha\beta}$ is defined by Eq. (10).

Vector $\langle\mathbf{D}^{\text{NL}}\rangle$ is complex and the phases of its Cartesian components are, typically, different. This means that $\langle\mathbf{D}^{\text{NL}}\rangle$ is elliptically polarized. It is neither collinear with the incident field $\mathbf{E}_0$, nor with the average local field. This follows from the fact that we cannot neglect the interaction of nonlinear dipoles, since this interaction takes place at the fundamental frequency. Vector $\langle\mathbf{D}^{\text{NL}}\rangle$ is also different for different light polarizations, and so is the enhancement factor G_K.

If the nonlinear molecules are in vacuum (i.e., there are no interactions between the dipoles), then the average dipole moment is collinear with the applied field,

$$\langle\mathbf{D}_0^{\text{NL}}\rangle=c|E_0|^2\mathbf{E}_0. \qquad (68)$$

Now we compare the values of $\langle D_\beta^{\text{NL}}\rangle$ and the amplitude of $\langle\mathbf{D}_0^{\text{NL}}\rangle$ for the case when β does not coincide with the polarization direction α of the applied field. We introduce the enhancement factors in the plane perpendicular to the direction of polarization, α:

$$G_{K,\alpha\beta}=\frac{Z(\omega)\langle|E|^2E_\gamma\alpha_{\gamma\beta}(\omega)\rangle}{|E_0|^2E_0}, \quad \beta\neq\alpha, \qquad (69)$$

for α polarization of $\mathbf{E}_0$. For $G_{K,\alpha\beta}$, the subscript α indicates the direction of the light polarization, whereas the subscript β gives the one of the Cartesian components of $\langle\mathbf{D}^{\text{NL}}\rangle$ in Eq. (69). The origin of such tensor structure of the enhancement is physically transparent. The system that we consider is not homogeneous and isotropic, so that the structural anisotropy results in excitation of nonlinear dipole moments in the directions different from the light polarization direction.

We also introduce enhancement factors for the projection of the nonlinear dipole on the polarization direction of the incident light as

$$G_{K,\alpha\alpha} = \frac{\langle |\mathbf{E}|^2 (\mathbf{E} \cdot \mathbf{E}) \rangle}{|E_0|^2 (\mathbf{E}_0 \cdot \mathbf{E}_0)}. \tag{70}$$

A similar expression was derived differently (by using the microscopic approach and Maxwell equations) in Ref. 38.

Note that a simple relation between the enhancements for DFWM and the Kerr effect follows from Eqs. (55) and (70):[6]

$$G_{DFWM} = |G_{K,\alpha\alpha}|^2. \tag{71}$$

Now we generalize our approach to the case when the films that compose the material are arbitrarily oriented in space; this is also equivalent to the case when the applied field has random polarization. Without any preferred direction, all the enhancement factors $G_{K,\alpha\alpha}$ are equiprobable, on average. Thus, the value of the average enhancement factor is given by

$$\langle G_K \rangle = \frac{1}{3} \left\langle \sum_\alpha G_{K,\alpha\alpha} \right\rangle. \tag{72}$$

VI. NUMERICAL CALCULATIONS

In this section we present results of numerical simulations for silver self-affine films. The enhancement coefficients are calculated based on formulas derived in Secs. IV and V. The experimental data[22] for the dielectric permittivity of silver are used to calculate the parameter $Z(\lambda)$ using Eqs. (6) and (7). The characteristic monomer's size R_m is set to be 5 nm, which is a typical value for silver nanocomposites.

A. Optical nonlinearities in films of different sizes

Because the enhancement factors introduced in Secs. IV and V are defined by the collective linear and nonlinear excitations of films, one might think that these factors depend on the average number of monomers (dipoles) in a film or, in other words, on the average film size.

To address this question, we generated several different ensembles (for details of the algorithm, see Sec. III B). The maximum linear size was 14×14 lattice units. Taking samples of bigger linear sizes would violate the quasistatic approximation that we used to derive the enhancement factors in previous sections.

We found that the enhancement coefficients did not show any systematic dependence on the linear size of the films (starting from 4×4 lattice units), and were the same within statistical errors for all the ensembles. This observation allows us to conclude that in the quasistatic limit, the nonlinear properties of rough self-affine structures do not depend on the linear size of a system or the number of monomers. Note that the same property was observed earlier for linear optical responses of self-affine surfaces.[5]

B. Giant enhancements of optical nonlinearities

In Fig. 3, we show the averaged (over 12 different film samples) enhancement factor for SHG from a self-affine surface; the enhancement was calculated using formulas (38)
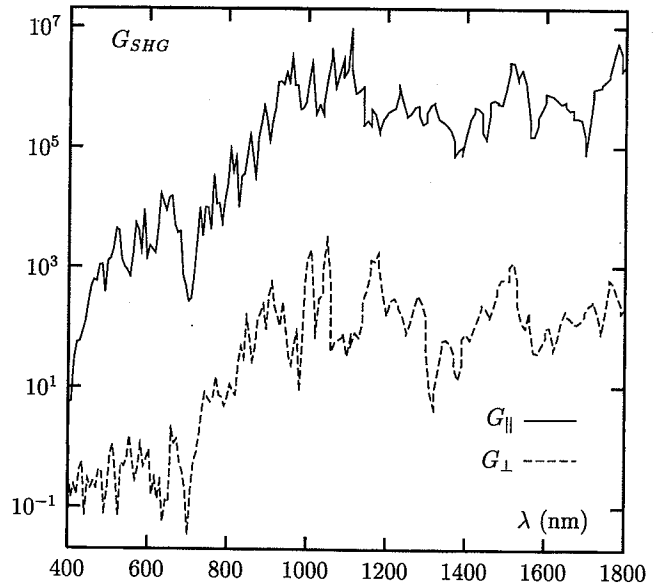

FIG. 3. The average enhancement factors for SHG from a self-affine silver surface, for the light polarized in the (x,y) plane of the film $(G_{SHG} \equiv G_{\|})$ and in the normal z direction $(G_{SHG} \equiv G_\perp)$.

and (39), for p and s polarizations, respectively. We plot our results for $\Gamma = 2$ ($a = b$). Note that real values of Γ indicate absence of nonlinear absorption by molecules.[39] We also obtained a number of curves for different values of b/a $\in [10^{-2}, 10]$ [see Eq. (34)]. We found that for different numerical values of Γ, the enhancement factors G are similar in terms of their magnitudes and spectral dependences (the results are not shown). This is in agreement with the fact that the spectral dependence of linear dipoles in Eq. (11) does not correlate with the value of Γ chosen to be independent of the incident wavelength.

We see that the anticipated inequality $G_\| \gg G_\perp$ holds, since the linear dipoles and corresponding local fields in Eq. (11) are, on average, larger for the incident field polarized in the plane of the film than in the normal direction; this is because a thin film can be roughly thought of as an oblate spheroid with a high aspect ratio. The largest average enhancement for SHG is $\sim 10^7$.

We also note that contributions from the last terms in Eqs. (38) and (39), which are proportional to strongly fluctuating (and changing their signs) products $E_x E_z$ and $E_y E_z$, are small and can be neglected with good accuracy. Also, in the short-wavelength part of the spectrum, when the interaction of the dipoles at 2ω can be neglected (because the surface modes are not excited), the diagonal element $\alpha_{zz}(2\omega)$ in Eqs. (38) and (39) dominates the off-diagonal ones, so that the local dipoles at 2ω are directed along the corresponding local fields at 2ω. In contrast, in the long-wavelength part of the spectrum, when the oscillations at 2ω lie within the surface mode band, the largest dipoles at 2ω are excited for the light polarized in the plane of the film, and therefore, the off-diagonal elements $\alpha_{zx}(2\omega)$ and $\alpha_{zy}(2\omega)$ are larger than $\alpha_{zz}(2\omega)$. These arguments allow one to simplify the general expressions (38) and (39), when they are used in the corresponding limiting cases.

In Fig. 4, we show the enhancement factor for THG, G_{THG}, calculated using formula (46). The values of G_{THG}
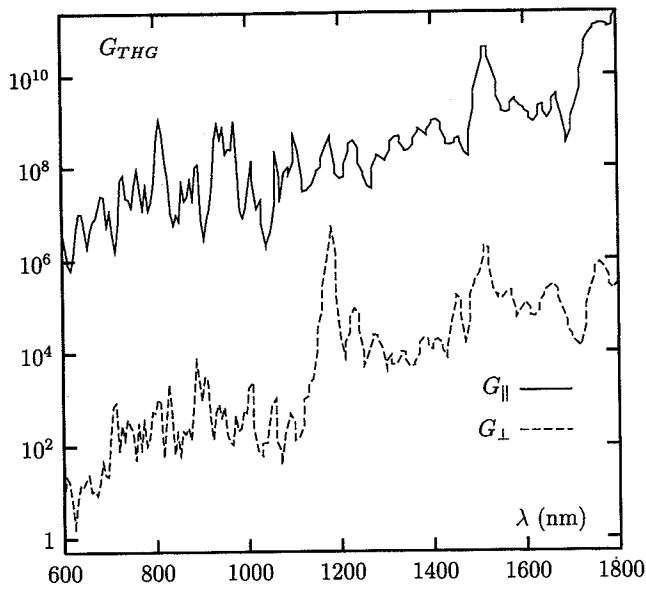
FIG. 4. The average enhancement factors for THG from a self-affine silver surface, for the light polarized in the (x,y) plane of the film $(G_{THG} \equiv G_{\parallel})$ and in the normal z direction $(G_{THG} \equiv G_{\perp})$.

field enhancements at the fundamental frequency, $g = |\langle E \rangle / E_0|^2$ and for the local enhancements of SHG and THG, $g_{SHG} = |d_i^{NL}(2\omega)|^2 / |d_0^{NL}(2\omega)|^2$ and $g_{THG} = |d_i^{NL}(3\omega)|^2 / |d_0^{NL}(3\omega)|^2$. The interactions of the nonlinear dipoles at the generated frequency is taken into account for both SHG and THG effects. The distributions of local enhancements are calculated for two wavelengths, 1 μm and 10 μm, for the light polarized in the plane of the film. As was discussed above, the largest average enhancements are achieved in the infrared region for the s-polarized incident light.

In the counterplots of Figs. 5 and 6, the white spots correspond to higher intensities whereas the dark areas represent the low-intensity zones. We can see that spatial positions of the "hot" and "cold" spots in the local enhancements at the fundamental and generated frequencies are localized in small spatially separated parts of the film. Since the fundamental and generated frequencies are different, the fundamental and generated waves excite different optical modes of the film surface and, therefore, produce different local-field distributions. With the frequency alternation, the locations of the "hot" and "cold" change for all the fields at the fundamental and generated frequencies. Thus different waves involved in the nonlinear interactions in a self-affine thin film produce nanometer-sized "hot" spots spatially separated for different waves. A similar effect was previously shown for Raman scattering from self-affine films.[12]

The values of the local-field intensities in Figs. 5 and 6 grow with the wavelength. The highest local enhancement

are even larger than for G_{SHG}, reaching $\sim 10^{11}$ values. The THG involves higher power of electric fields, so that the dominance of local fields E_i over E_0 leads to larger values of enhancement factors.

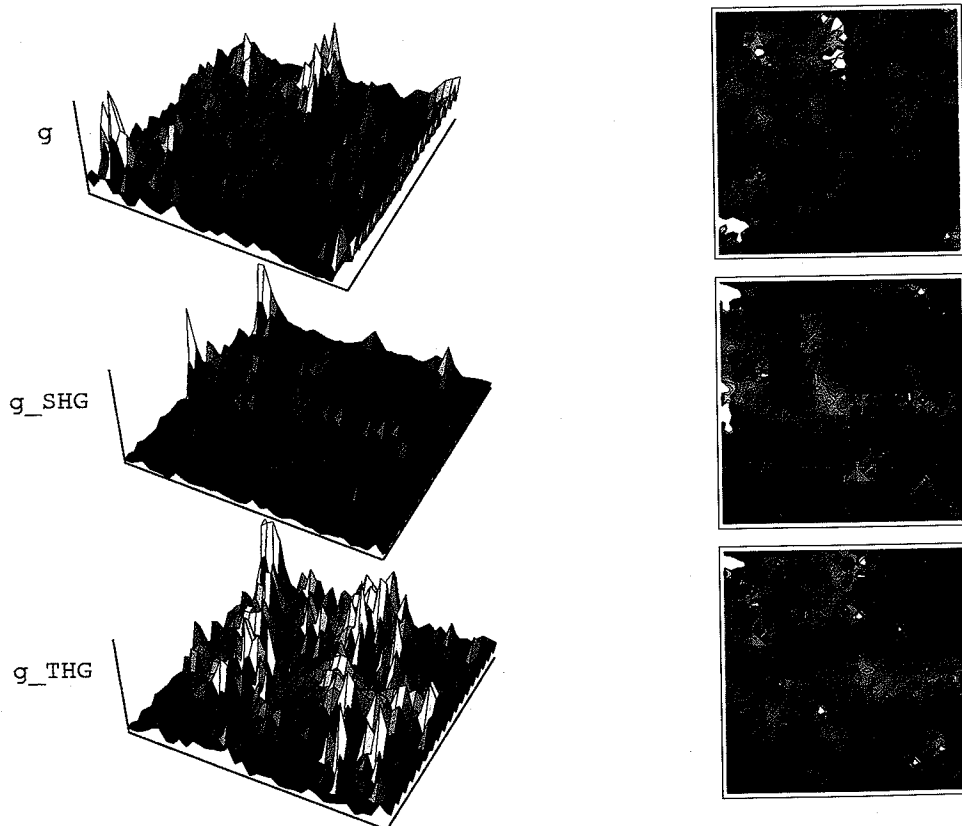In Figs. 5 and 6, we plot spatial distributions for local-

FIG. 5. Spatial distributions of the local enhancements for the field at the fundamental wavelength, g, for SHG signal, g_{SHG}, and for THG signal, g_{THG}. The corresponding counter plots for the spatial distributions are also shown in all cases. The fundamental wavelength is $\lambda = 1$ μm. The linear scales are used in all cases. The highest enhancement values in the figures are as follows: $g = 5 \times 10^3$, $g_{SHG} = 5 \times 10^8$, and $g_{THG} = 2 \times 10^{12}$.
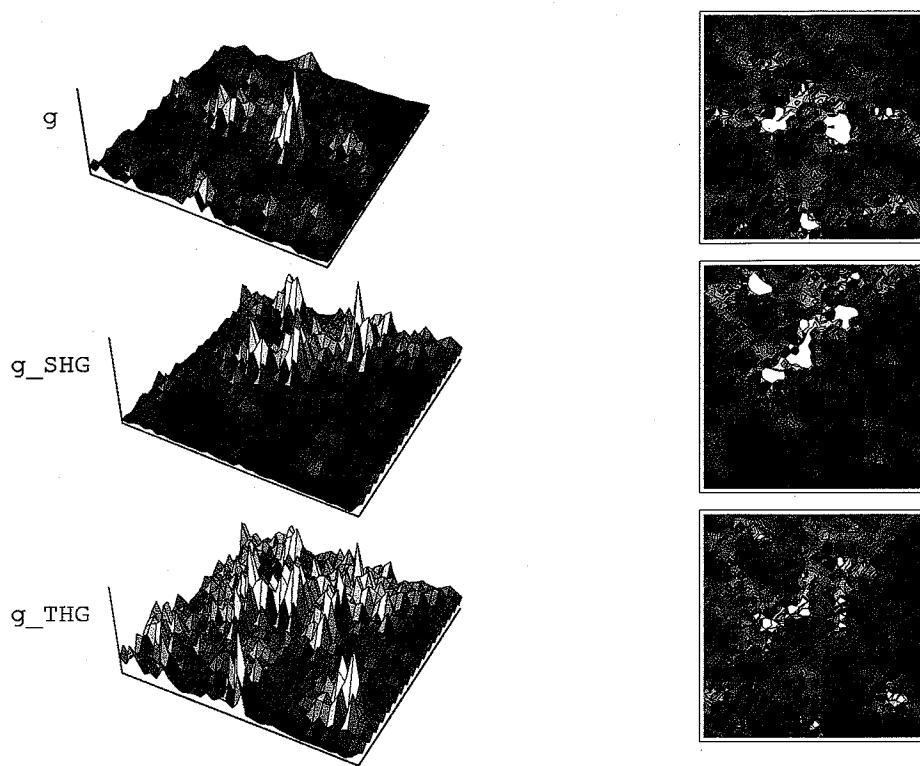
FIG. 6. Same as Fig. 5, but for $\lambda = 10$ μm. The highest enhancement values are as follows: $g = 3 \times 10^4$, $g_{SHG} = 10^{13}$, and $g_{THG} = 2 \times 10^{19}$.

factor in the spatial distribution g changes from 5×10^3 at $\lambda = 1$ μm to 3×10^4 at $\lambda = 10$ μm. For the SHG and the THG spatial distributions, the maximum increases from 5×10^8 to 10^{13} and from 2×10^{12} to 2×10^{19}, respectively. Such behavior correlates with the fact that the average enhancement factor increases toward the infrared spectral region. We emphasize that the local enhancements can exceed the average one by several orders of magnitude. For example, comparison of the maximum local enhancement with the average enhancement for $\lambda = 1$ μm shows that the maximum intensity peaks exceed the average intensity by approximately 2 orders of magnitude for SHG (cf. Figs. 3 and 5) and by 4 orders of magnitude, for THG (cf. Figs. 4 and 5). This occurs, in part, due to the fact that the spatial separation between the hot spots can be significantly larger than their characteristic sizes, and also due to destructive interference between the generated fields in different peaks.

The giant local enhancements of nonlinear processes (e.g., up to 10^{19} for THG at 10 μm) open a fascinating possibility of the fractal-surface-enhanced nonlinear optics and spectroscopy of single molecules. Also, if the near-field scanning optical microscopy is employed, nonlinear nano-optics and nanospectroscopy (with nanometer spatial resolution) become possible. In contrast, with the conventional far-zone optics only the average enhancement of optical processes can typically be measured.

The huge average enhancement for DFWM on a self-affine film is illustrated in Fig. 7. The larger values of enhancement for DFWM, compared to THG, are explained by the fact that the interaction of nonlinear dipoles is stronger when the generated frequency is equal to the fundamental one. Also, the role of destructive interference for the field

generated in different points is much larger for high-order harmonic generation than for DFWM.

In Figs. 8(a) and 8(b), we show the calculated real and imaginary parts of the Kerr enhancement factor. We calculated the enhancements using formulas (69) and (70). The enhancement factors $G_{K,\alpha\beta}$ for the incident light polarized parallel to the film's plane ($\alpha = x, y$) are the largest, and approximately equal to each other for $\beta = x, y$, i.e., $|G_{K,xx}| \approx |G_{K,yy}| \approx |G_{K,xy}| \approx |G_{K,yx}|$. Note, however, that the signs
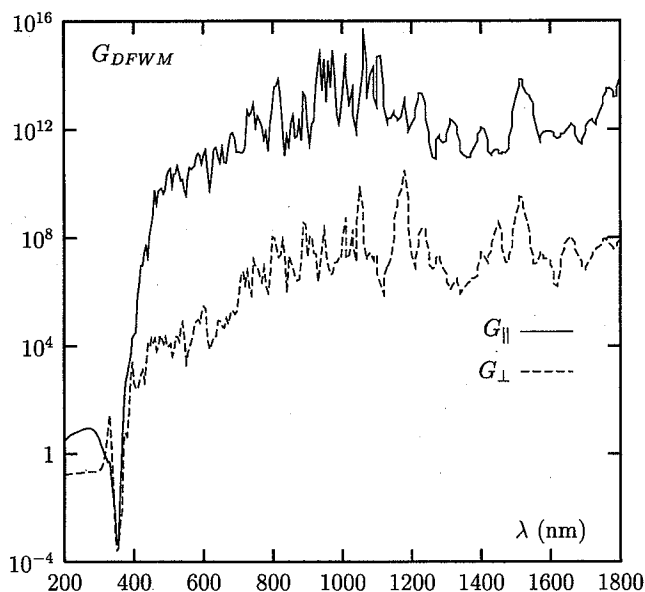

FIG. 7. The average DFWM enhancement factors from a self-affine silver surface, for the light polarized in the (x, y) plane of the film ($G_{DFWM} \equiv G_{\parallel}$) and in the normal z direction ($G_{DFWM} \equiv G_{\perp}$).
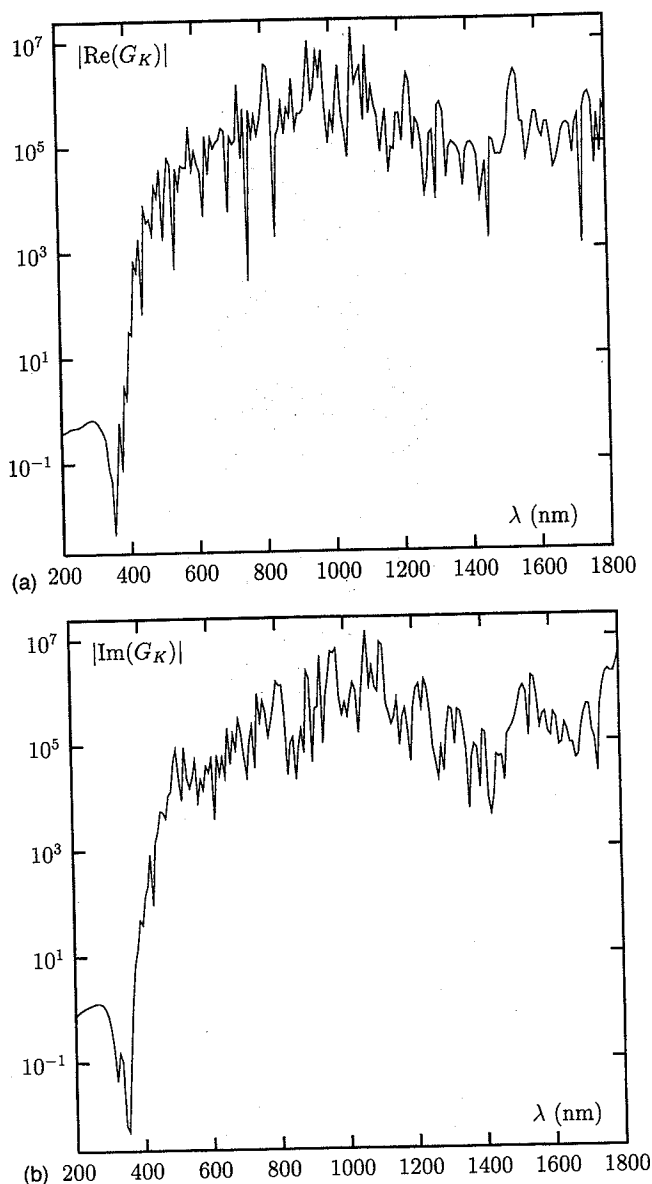
$G_K = \Sigma_{\alpha,\beta=x,y} G_{K,\alpha\beta}/4$. The calculations show that $|\mathrm{Re}(G_K)| \sim |\mathrm{Im}(G_K)|$, and both are especially large (up to $\sim 10^7$) in the near-infrared. With the calculated $G_K(\lambda)$, spectral dependences for the nonlinear corrections to absorption and refraction can be found using formulas (61), (62), and (65) and the λ dependence of the "seed" nonlinear susceptibility $\chi^{(3)}$.

VII. SUMMARY AND CONCLUDING REMARKS

In this paper nonlinear optical effects on rough surfaces of metal films were studied in the quasistatic approximation. The spectral dependence of the average enhancement factors for optical nonlinearities on a silver self-affine surface was calculated in a wide spectral range. The average enhancements are very large, reaching values of up to 10^7 and 10^{15} for the second- and third-order nonlinear optical processes, respectively. The huge enhancements are due to excitation of strongly inhomogeneous dipolar modes of a self-affine film.

In addition to the average enhancement factors, we calculated the spatial distributions of the local enhancements on the surface. In certain areas the local enhancements can exceed the average ones by several orders of magnitude. The existence of these extremely high peaks in the local generated signals ("hot" spots) makes feasible the nonlinear optical probing of single molecules adsorbed on the self-affine surface of a thin film.

The spatial distributions of local enhancements for the second and the third harmonic generation were calculated for the wavelengths 1 μm and 10 μm. It is shown that maximums of the local enhancements at the fundamental and generated frequencies are spatially separated on the surface. The spatial positions of the "hot" spots at the fundamental and generated frequencies are different because they resonate, in general, with different surface modes. The spatial positions of the "hot" spots change with the wavelength of the applied field.

The observed giant enhancements are related to the surface fractal geometry. In self-affine thin films, optical excitations tend to be localized in small subwavelength regions, so that the local fields fluctuate strongly on the surface of the film. A typical pattern of the local field distribution consists of a number of high peaks separated by distances larger than the characteristic peak sizes. Such field distributions can be detected in the near-zone region, whereas the average (over the whole surface) enhancement factors are registered in the far zone. The recent developments in experimental methods of the near-field scanning optical microscopy make possible measurements of local fields, including nonlinear ones, with the subwavelength resolution.[15,40]

FIG. 8. The absolute values of the real $|\mathrm{Re}(G_K)|$ and imaginary $|\mathrm{Im}(G_K)|$ parts of the average enhancement factors for the Kerr-nonlinearity for the light polarized in the (x,y) plane of the film (see the text for details).

of both $\mathrm{Re}(G_{K,\alpha\beta})$ and $\mathrm{Im}(G_{K,\alpha\beta})$ can be different for different tensor components and strongly vary with λ. This means that for some λ, the α-polarized incident light can undergo self-focusing in, say, the x direction and defocusing in the y direction; the situation can be reversed for some other wavelength. Similarly, competition between different modes may result in both positive and negative corrections to the resultant nonlinear absorption, depending on the polarization and wavelength of the applied field. These interesting properties can be important for various applications of rough thin films, for example, as photonic devices, such as optical switches.

In Figs. 8(a) and 8(b), we plot the absolute values of the real and imaginary parts of G_K defined, for simplicity, as

*Also with the Institute of Automation and Electrometry, Siberian Branch of the Russian Academy of Science, 630090 Novosibirsk, Russia.

†Author to whom correspondence should be addressed. Electronic address: vshalaev@nmsu.edu

[1] *Electron Transport and Optical Properties of Inhomogeneous Media*, edited by J. C. Garland and D. B. Tanner (AIP, New York, 1978); *Electron Transport and Optical Properties of Inhomogeneous Media* (*ETOPIM 3*), edited by W. L. Mochan and R.G. Barrera (North-Holland, Amsterdam, 1994).

[2] J. Feder, *Fractals* (Plenum Press, New York, 1988).

[3] R. Chiarello, V. Panella, J. Krim, and C. Thompson, Phys. Rev. Lett. **67**, 3408 (1991); J. Krim, I. Heyvaert, C. Van Haesendonck, and Y. Bruynseraede, *ibid.* **70**, 57 (1993).

[4] C. Douketis, Z. Wang, T. L. Haslett, and M. Moskovits, Phys. Rev. B **51**, 11 022 (1995).

[5] V. M. Shalaev, R. Botet, J. Mercer, and E. B. Stechel, Phys. Rev. B **54**, 8235 (1996).

[6] V. M. Shalaev, Phys. Rep. **272**, 61 (1996); V. A. Markel, V. M. Shalaev, E. B. Stechel, W. Kim, and R. L. Armstrong, Phys. Rev. B **53**, 2425 (1996); V. M. Shalaev, E. Y. Poliakov, and V. A. Markel, *ibid.* **53**, 2437 (1996).

[7] V. A. Markel, L. S. Muratov, M. I. Stockman, and T. F. George, Phys. Rev. B **43**, 8183 (1991); M. I. Stockman, L. N. Pandey, and T. F. George, *ibid.* **53**, 2183 (1996).

[8] For a spheroid, there are three nondegenerate resonances with non-zero total dipole moment.

[9] *Surface Enhanced Raman Scattering*, edited by R. K. Chang and T. E. Furtak (Plenum Press, New York, 1982).

[10] E. M. Purcell and C. R. Pennypacker, Astrophys. J. **186**, 705 (1973).

[11] B. T. Draine, Astrophys. J. **333**, 848 (1988).

[12] E. Y. Poliakov, V. M. Shalaev, V. A. Markel, and R. Botet, Opt. Lett. **21**, 1628 (1996).

[13] V. M. Shalaev, E. Y. Poliakov, V. A. Markel, and R. Botet, in *Fractal Frontiers*, edited by M. M. Novak (World Scientific, Singapore, 1997); V. M. Shalaev, E. Y. Poliakov, V. A. Markel, and R. Botet, Physica A **241**, 249 (1997).

[14] V. M. Shalaev and A. K. Sarychev, Phys. Rev. B **57**, 13 265 (1998); F. Brouers, S. Blacher, A. N. Lagarkov, A. K. Sarychev, P. Gadenne, and V. M. Shalaev, Phys. Rev. B **55**, 13 234 (1997); P. Gadenne, F. Brouers, V. M. Shalaev, and A. K. Sarychev, J. Opt. Soc. Am. B **15**, 68 (1998).

[15] E. Betzig and J. K. Trautman, Science **257**, 189 (1992).

[16] P. Chappetta, J. Phys. A **13**, 2101 (1980); D. Keller and C. Bustamente, J. Chem. Phys. **84**, 2961 (1986).

[17] S. B. Singham and C. F. Bohren, J. Opt. Soc. Am. A **5**, 1867 (1988).

[18] M. K. Singham, S. B. Singham, and G. C. Salzman, J. Chem. Phys. **85**, 3807 (1986); P. J. Flatau, G. L. Stephens, and B. T. Draine, J. Opt. Soc. Am. A **7**, 593 (1990); C. E. Dungley and C. F. Bohren, *ibid.* **8**, 81 (1991).

[19] M. V. Berry and I. C. Percival, Opt. Acta **33**, 577 (1986).

[20] V. M. Shalaev, R. Botet, and R. Jullien, Phys. Rev. B **44**, 12 216 (1991).

[21] J. J. Jackson, *Classical Electrodynamics* (Wiley, New York, 1975).

[22] P. B. Johnson and W. Christy, Phys. Rev. B **6**, 3470 (1972).

[23] M. Kardar, G. Parisi, and Y. C. Zhang, Phys. Rev. Lett. **56**, 889 (1986).

[24] P. Meakin, P. Ramanlal, L. M. Sander, and R. C. Ball, Phys. Rev. A **34**, 5091 (1986).

[25] J. M. Kim and J. M. Kosterlitz, Phys. Rev. Lett. **62**, 2289 (1989).

[26] N. Bloembergen and P. S. Pershan, Phys. Rev. **128**, 606 (1962).

[27] Y. R. Shen, *The Principles of Nonlinear Optics* (Wiley, New York, 1984).

[28] G. L. Richmond, J. M. Robinson, and V. L. Shanon, Prog. Surf. Sci. **28**, 1 (1988).

[29] S. Janz and H. M. van Driel, Int. J. Nonlinear Opt. Phys. **2**, 1 (1993).

[30] J. E. Sipe, V. C. Y. So, M. Fukui, and G. I. Stegeman, Phys. Rev. B **21**, 4389 (1980); P. Guyot-Sionnest, W. Chen, and Y. R. Shen, *ibid.* **33**, 8254 (1986).

[31] R. Murphy, M. Yeganeh, K. J. Song, and E. W. Plummer, Phys. Rev. Lett. **63**, 318 (1989); O. A. Aktsipetrov, A. A. Nikulin, V. I. Panov, and S. I. Vasil'ev, Solid State Commun. **73**, 411 (1990); H. Ishida and A. Liebsch, Phys. Rev. B **50**, 4834 (1994); A. V. Petukhov and A. Liebsch, Surf. Sci. **334**, 195 (1995).

[32] P. S. Pershan, Phys. Rev. Lett. **130**, 919 (1963); P. Guyot-Sionnest and Y. R. Shen, Phys. Rev. B **38**, 7985 (1988).

[33] B. S. Mendoza and W. L. Mochan, Phys. Rev. B **53**, 4999 (1996).

[34] J. Rudnick and E. A. Stern, Phys. Rev. B **4**, 4274 (1971).

[35] Note that in this simplified model the orientation of **n** does not change from site to site.

[36] O. A. Aktsipetrov, O. Keller, K. Pedersen, A. A. Nikulin, N. N. Novikova, and A. A. Fedyanin, Phys. Lett. A **179**, 149 (1993).

[37] R. W. Boyd, *Nonlinear Optics* (Academic Press, New York, 1992).

[38] D. J. Bergman and D. Stroud, Solid State Phys. **46**, 147 (1992).

[39] Our calculations show that complex values of Γ do not change significantly the enhancement profile.

[40] D. P. Tsai, J. Kovacs, Z. Wang, M. Moskovits, V. M. Shalaev, J. Suh, and R. Botet, Phys. Rev. Lett. **72**, 4149 (1994); V. M. Shalaevf and M. Moskovits, *ibid.* **75**, 2451 (1995).